Rare Met. (2017) 36(8):627–634
DOI 10.1007/s12598-016-0785-5

RARE METALS
www.editorialmanager.com/rmet

Corrosion behavior of Al–3.0 wt%Mg alloy in NaCl solution under magnetic field

Xin Zhang, Ze-Hua Wang*, Ze-Hua Zhou, Jian-Ming Xu, Zhao-Jun Zhong, Huan-Long Yuan

Received: 29 July 2015 / Revised: 5 September 2015 / Accepted: 3 June 2016 / Published online: 29 June 2016

Abstract The influences of applied magnetic field on the corrosion behavior of Al–3.0 wt%Mg alloy in 3.5 wt% NaCl solution were investigated by electrochemical measurements, scanning electron microscopy (SEM) and energy-dispersive spectroscopy (EDS). Stochastic analysis was applied to investigate the influences of applied magnetic field. The results indicate that the application of horizontal magnetic field of 0.4 T would increase the pitting corrosion potential (E_{pit}), decrease the corrosion current density (i_{corr}), prolong the pit initiation time, slow down the pit generation rate and inhibit the growth of pitting of the tested alloys in 3.5 wt% NaCl solution. The applied magnetic field would also change the mechanism of pit initiation of Al–3.0 wt%Mg alloy from A_3 model (without magnetic field) to $A_3 + A_4$ model (with magnetic field). The intermediate product $Al^{+}_{(ad)}$ is the paramagnetic ion that would be influenced by magnetic field sensitively.

Keywords Al–3.0 wt%Mg alloy; Applied magnetic field; Pitting corrosion; Paramagnetic ion

X. Zhang, Z.-H. Wang*, Z.-H. Zhou, Z.-J. Zhong, H.-L. Yuan
College of Mechanics and Materials, Hohai University, Nanjing 210098, China
e-mail: zhwang@hhu.edu.cn

J.-M. Xu
Zhangjiagang Hongji Aluminum Co. Ltd., Suzhou 215600, China

1 Introduction

Al–Mg alloys, because of their good comprehensive properties including low resistivity, high specific strength and excellent corrosion resistance, are considered as the ideal electromagnetic shielding material and even are used as substitutes for some rare metallic materials [1–4]. Because of their excellent corrosion resistance, Al–Mg alloys can be specified as outdoor applications. Al–Mg electromagnetic shielding wire is served in magnetic field; however, the influence of this special environment on its corrosion behavior is not clear and lack of research.

Up to now, the effects of magnetic fields on electrochemical corrosion behavior of metallic materials in aqueous solutions have been mainly focused on electrodeposition of metals and ferromagnetic electrodes. Many studies revealed that magnetic field could influence the dissolution of iron, while many disputed observations have been reported [5–10]. The applied magnetic field accelerated the corrosion process of copper and titanium in low NaCl concentration and suppressed the corrosion rates of copper and zinc in nitric acid [11–14]. Although a large numbers of reports mentioned the effect of magnetic fields on the corrosion behaviors of metallic materials, few reports were related to Al–Mg alloys relatively.

It is well known that Al–Mg alloys, especially those with high Mg content, are susceptible to pitting corrosion. So, in this paper, the electrochemical corrosion and pitting corrosion behaviors of Al–3.0 wt%Mg alloy under applied magnetic field of 0.4 T in 3.5 wt% NaCl solution were investigated. The influence mechanism of magnetic field on the electrochemical characteristics and pitting corrosion characteristics of tested alloys were discussed.

2 Experimental

2.1 Material preparation

A_{00} aluminum ingot (99.7 wt% Al) was melted at 720 °C in a graphite crucible by electrical resistance furnace. The pure magnesium ingot was then added into the molten aluminum. The degassing was conducted with argon for 10 min before pouring at 720 °C. Owing to the poor fluidity of Al–3.0 wt%Mg molten, the alloys were cast into the metal mold with a big riser. The specimens were machined to the dimension of 10 mm × 10 mm × 10 mm. The surfaces of the specimens were polished before testing.

2.2 Electrochemical measurement

The corrosion process of the alloys was evaluated by electrochemical test by CHI660E A14330 electrochemical workstation. The test was conducted in unsaturated 3.5 wt% NaCl solution according to ASTM G1-03. Test was carried out with specimen as working electrode, the 232 model saturated calomel electrode as reference electrode and the 213 model Pt wire as auxiliary electrode. A horizontal magnetic field of 0.4 T was applied by Nd–Fe–B permanent-magnet, as shown in Fig. 1.

Four kinds of electrochemical tests, namely open circuit potential (OCP) test, potentiodynamic polarization test, electrochemical impendence spectroscopy (EIS) test and potentiostatic current response test, were made according to ASTM G3-13. The immersion time of OCP tests was 10 min. As the OCP became steady, EIS tests were conducted by applying the sinusoidal potential excitation amplitude of 5 mV to the OCP with a frequency ranging from 100 kHz to 10 mHz. Potentiodynamic polarization curves were recorded at a sweep rate of 1 $mV \cdot s^{-1}$. The corrosion current density (i_{corr}), corrosion potential (E_{corr}) and pitting corrosion potential (E_{pit}) were calculated according to the Tafel extrapolation technique. The potentiostatic current response test included passivating and pitting corrosion inducing. The specimens were passivated in 0.01 $mol \cdot L^{-1}$ NaOH solution for 500 s under a potentiostatic voltage of −0.85 V. Then, the pitting corrosion inducing experiment was continued in 3.5 wt% NaCl solution and the current–time curves were obtained when the frequency of potentiostatic current response was 5 Hz. When the current reached 1 mA, the test finished. The potentiodynamic polarization test and potentiostatic current response test were repeated twenty times.

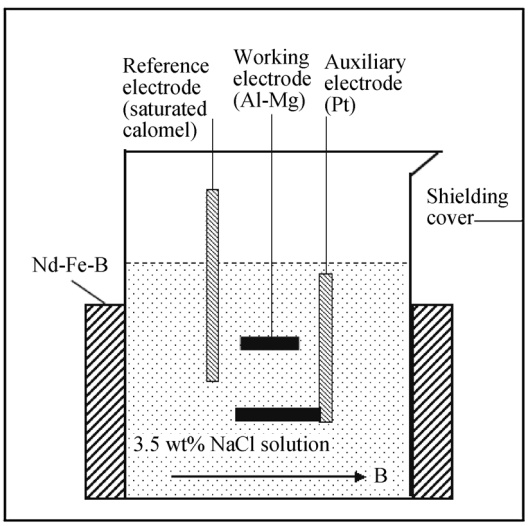

Fig. 1 Placement of electrodes and magnetic field

2.3 Immersion test

The specimens were kept in 3.5 wt% NaCl solution with and without an applied magnetic field during the immersion test. The total duration of the corrosion test lasted for 600 h. Surface morphologies of the specimens were observed by scanning electron microscopy (SEM, Hitach S-3400 N). The amount and dimension of pitting holes were calculated. Local composition was analyzed by energy-dispersive spectroscopy (EDS, Horiba EX250).

3 Results

3.1 Polarization measurements

Figure 2 shows potentiodynamic polarization curves and pitting corrosion potential (E_{pit}) of Al–3.0 wt%Mg alloy with and without magnetic field. Their corrosion potential (E_{corr}) and corrosion current density (i_{corr}) are inset in Fig. 2a. The applied magnetic field would make E_{pit} shift toward negative direction from −1.0520 to −1.0821 V. The corrosion current density (i_{corr}) of the alloys under magnetic field is 4.705 $\mu A \cdot cm^{-2}$, which is lower than that of without magnetic field, 5.319 $\mu A \cdot cm^{-2}$. Similar potentiodynamic curves of the alloy in NaCl solution with and without magnetic field are presented. Both of them have a passivation area with a same current. The applied magnetic field (0.4 T) could increase E_{pit} of Al–3.0 wt%Mg alloys from −0.9033 to −0.8283 V, and of course, it increases the stability of the passive films.

Figure 2b shows the cumulative probability (P) of E_{pit} values of Al–3.0 wt%Mg alloy with and without magnetic field.

$$P = i/(1+N), \quad i = 1, 2, 3, \ldots N \tag{1}$$

where N is the number of experimental times. E_{pit} values are represented in linear distributions both with and without magnetic field. An applied magnetic field makes the

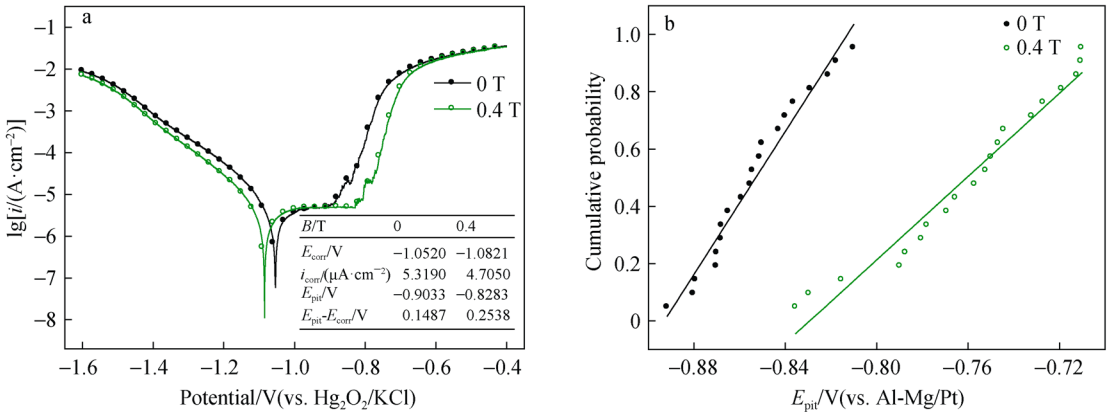

Fig. 2 Potentiodynamic polarization characteristic of Al–3.0 wt%Mg alloy: **a** potentiodynamic polarization curves and **b** distribution of E_{pit} values

line of E_{pit} values move. It means that the applied magnetic field would increase the pitting corrosion potential and decrease the corrosion current density of Al–3.0 wt%Mg alloy in 3.5 wt% NaCl solution.

3.2 Impedance spectroscopy

The influence of applied magnetic field on corrosion behavior of Al–3.0 wt%Mg alloys in 3.5 wt% NaCl solution was further verified by EIS test. Figure 3 shows Nyquist diagram of the alloys when the magnetic field was applied or not, where Z_{Re} and Z_{Im} are the real and imaginary parts of impedance, respectively. Both of impedance spectra show capacitive circles at high frequency and diffusible lines at low frequency, but the diameters of the capacitive circles are different. The applied magnetic field could reduce the diagram of the capacitive circle of Al–3.0 wt%Mg alloy, as shown in Fig. 3. As known, the diameter of the capacitive circle is associated with the

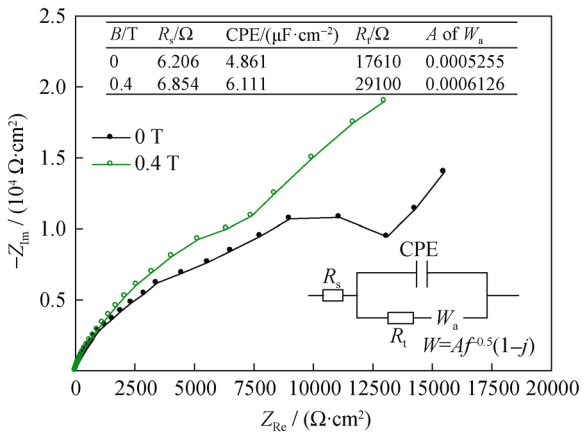

Fig. 3 Nyquist diagram of Al–3.0 wt%Mg alloy in absence and presence of magnetic field

charge transfer resistance. The bigger the diameter of the capacitive circle is, the slower the corrosion rate is. So, the result of Fig. 3 indicates that the applied magnetic field could reduce the corrosion rate of Al–3.0 wt%Mg alloy in 3.5 wt% NaCl solution.

An equivalent circuit inset in Fig. 3 is obtained by ZSimpwin commercial software to fit the experimental Nyquist plots. In this case, R_s, R_t, CPE and W_a represent the solution resistance, the charge transfer resistance, the capacitance of the double layer and Warburg resistance, respectively. As for the formula $W = Af^{-0.5}(1 - j)$ in Fig. 3, W is the Warburg resistance, j is imaginary unit, f is angular frequency and A is the fixed coefficient. R_t value is influenced or determined by the ability of ionic conduction across the passive film. It is seen that under magnetic field, R_t value of the alloy is higher than that of without magnetic field, and it increases from 17,600 to 29,100 Ω with a 0.4 T magnetic field applied. It means that the magnetic field increases the resistance of ionic passing through the passive film on the surface of Al–3.0 wt%Mg alloy and makes the pitting corrosion difficult to proceed.

3.3 Current–time curves under constant potential

The pitting corrosion of aluminum alloy is considered as the combination of two steps: pit initiation and pit growth [15, 16]. Long pit initiation time would reduce the possibility of corrosion and low pit growth rate with short pit initiation time would result in uniform corrosion. Figure 4 shows current response curves of Al–3.0 wt%Mg alloy at a constant potential of −0.85 V. The current density decreases with the increase of test time at the beginning because the alloy is in a passive state in this period. Then, the current density turns to increase sharply when the passive film is punctured. The time from the start point to the break point is named as the pit initiation time. As

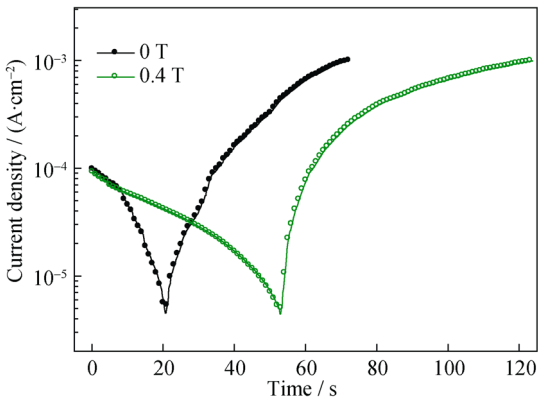

Fig. 4 Current responses of Al–3.0 wt%Mg alloy in absence and presence of magnetic field at a constant potential of −0.85 V

shown in Fig. 4, the pit initiation time of Al–3.0 wt%Mg alloy is about 53 s when it is corroded with a 0.4 T magnetic field. However, it is 20 s when the alloy is corroded without magnetic field. It means that an applied magnetic field would greatly increase the pit initiation time of Al–3.0 wt%Mg alloy corroded in 3.5 wt% NaCl solution.

The relationship between the Napierian logarithm of survival probability (P) and pit initiation time was recorded during parallel potentiostatic current response test, as shown in Fig. 5. Shibata et al. [17–19] established a statistical method to analyze the formation of pitting corrosion. The schematic illustration of survival probability ($\ln P$) vs time of various stochastic models is inset in Fig. 5, and the analytical expression of the survival probability function for various stochastic models is listed in Table 1, where λ (λ_1, λ_2 and λ_3 mean different λ values) is pit generation rate, μ is repassivation rate, t_0 is pit initiation time, t is the corrosion time, m and α are the fixed parameters in different formulae, f_i is the statistic parameter and τ_c is the repassivation time. The pit corrosion would be divided into two kinds of models: pit birth process (A) and pit birth and death process (B). According to Fig. 5, the pit initiation corrosion of the alloy is similar to Model A_3 of pit birth process when there is no magnetic field. The existence of 0.4 T magnetic field changes the pit initiation corrosion model to $A_3 + A_4$ model, and the pit generation rate (λ) decreases from 2.484×10^{-2} to 2.472×10^{-2} (λ_1) and 1.444×10^{-2} (λ_2). So an applied magnetic field would prolong the pit initiation time and slow down the pit generation rate.

Table 1 Analytical expression of survival probability function for various stochastic models

Model	Survival probability function
Birth process	
A_1	$P_{sur}(t) = \exp[-\lambda(t - t_0)]$
A_2	$P_{sur}(t) = \exp[-m\lambda(t - t_0)]$
A_3	$P_{sur}(t) = 1 - \{1 - \exp[-\lambda(t - t_0)]\}^m$
A_4	$P_{sur}(t) = \sum f_i \exp[-\lambda_i(t - t_0)]$
Birth and death process	
B_1	$P_{sur}(t) = \mu/(\lambda + \mu) + \lambda/(\lambda + \mu)\exp[-(\lambda + \mu)(t - t_0)]$
B_2	$P_{sur}(t) = \exp[-\alpha\lambda(t - \tau_c)\exp(-\mu\tau_c)]$

After the passive film was punctured, the current density increases sharply, as shown in Fig. 6, indicating that a stable pit is formed. The area of shadow region expresses electric quantity (Q) consumed during pit growing process. The stable pit growth rate (v) could be expressed by Q/t. And the stable pit growth time is calculated to be 32 s, which is determined by the shortest time from the beginning of the pitting corrosion to the finishing of the test among the 40 group data.

The parameter reduced variant (Y) of Gumble probability was calculated by formula:

$$Y = -\ln\{-\ln[1 - i/(N + 1)]\} \quad (2)$$

The plots of Gumble probability and stable pit growth rate of the alloy are shown in Fig. 7a. An applied magnetic field

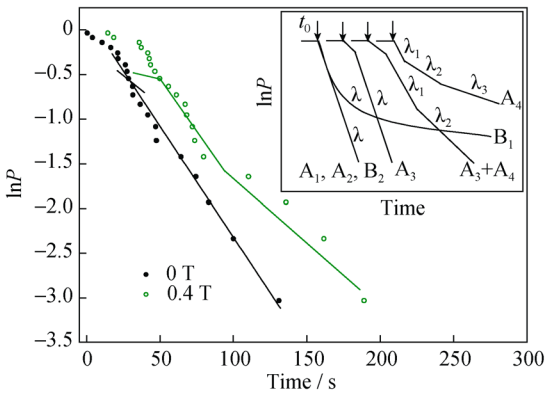

Fig. 5 Plots of survival probability and time of Al–3.0 wt%Mg alloy and various stochastic models

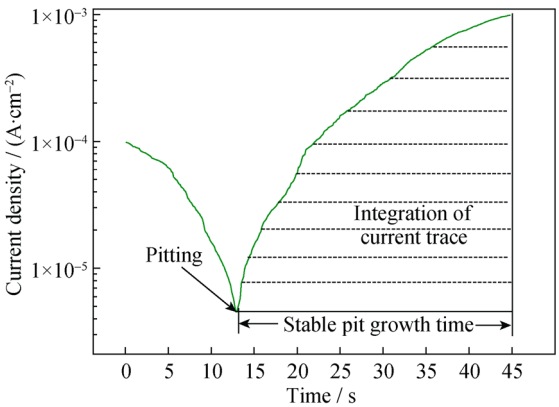

Fig. 6 Determination method of stable pit growth rate

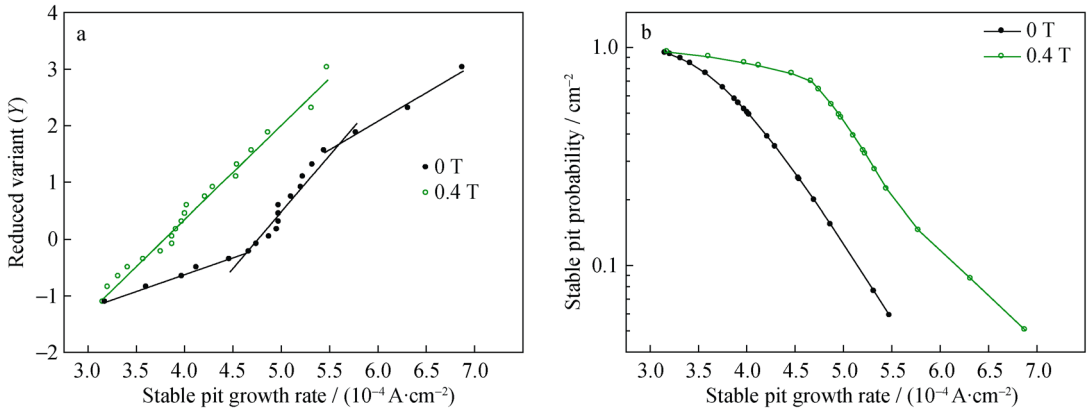

Fig. 7 Gumble probability plots and probabilities of various stable pit growth rate plots in absence and presence of magnetic field

Table 2 Typical Gumble distribution parameters at different magnetic intensities

Magnetic intensity (B)/T	Stable pits growth rate (v)/(A·cm^{-2})	Location parameters (δ)	Scale parameters (α)
0	$\leq 4.47 \times 10^{-4}$	3.790×10^{-4}	6.025×10^{-5}
	$4.47 \times 10^{-4} - 5.45 \times 10^{-4}$	5.052×10^{-4}	1.683×10^{-4}
	$5.45 \times 10^{-4} - 6.88 \times 10^{-4}$	4.759×10^{-4}	5.019×10^{-5}
0.4	$< 5.48 \times 10^{-4}$	3.933×10^{-4}	9.947×10^{-5}

changes the distribution of the stable pit growth rate of the alloy clearly. It presents in three segment distributions when there is no applied magnetic field, and it is a linear distribution when there is magnetic field. Location parameter (δ) and scale parameter (α) are obtained through the fitting of two curves in Fig. 7a and listed in Table 2. The probabilities of various stable pit growth rate were calculated by the following formula according to the parameter values in Table 2.

$$P = 1 - \exp\{-\exp[-(v - \delta)/\alpha]\} \quad (3)$$

The curves are shown in Fig. 7b. At the certain stable pit probability, the stable pit growth rate of the alloy under magnetic field is lower than that of the alloy without magnetic field. So, the magnetic field would reduce the growth of pitting of Al–3.0 wt%Mg alloy in 3.5 wt% NaCl solution.

3.4 Immersion test

During the immersion test of Al–3.0 wt%Mg alloy in 3.5 wt% NaCl solution, pitting holes would occur with the progress of the test going on. The number of corrosion pitting holes on the surface of Al–3.0 wt%Mg alloys was counted, as shown in Fig. 8. With the increase of immersion test time, the number of pitting holes increases both in the absence and presence of magnetic field addition. But the increasing rate of the pitting hole when the corrosion

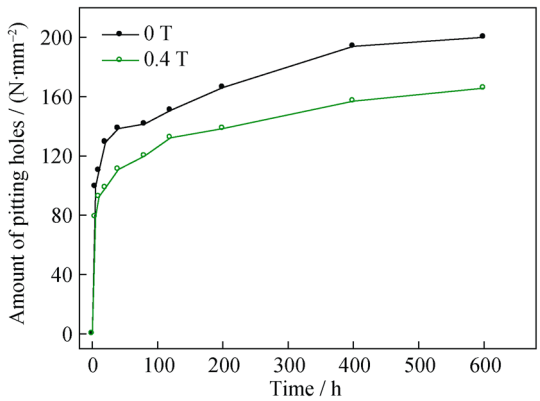

Fig. 8 Amount of pitting holes of Al–3.0wt%Mg alloys in 3.5 wt% NaCl solution tested in absence and presence of magnetic field

tested was conducted under magnetic field is much lower than that when the test was carried without magnetic field. It illustrates that the magnetic field would increase the pit initiation period or depresses the formation of the pitting hole. The result is consistent with electrochemical experiment.

After immersion test for 600 h in 3.5 wt% NaCl solution, many pitting holes occur on the surface of Al–3.0 wt%Mg alloy. Figure 9a, b shows SEM images of the corroded alloy. The amount of pitting holes on the surface of the alloy corroded under magnetic field of 0.4 T is less

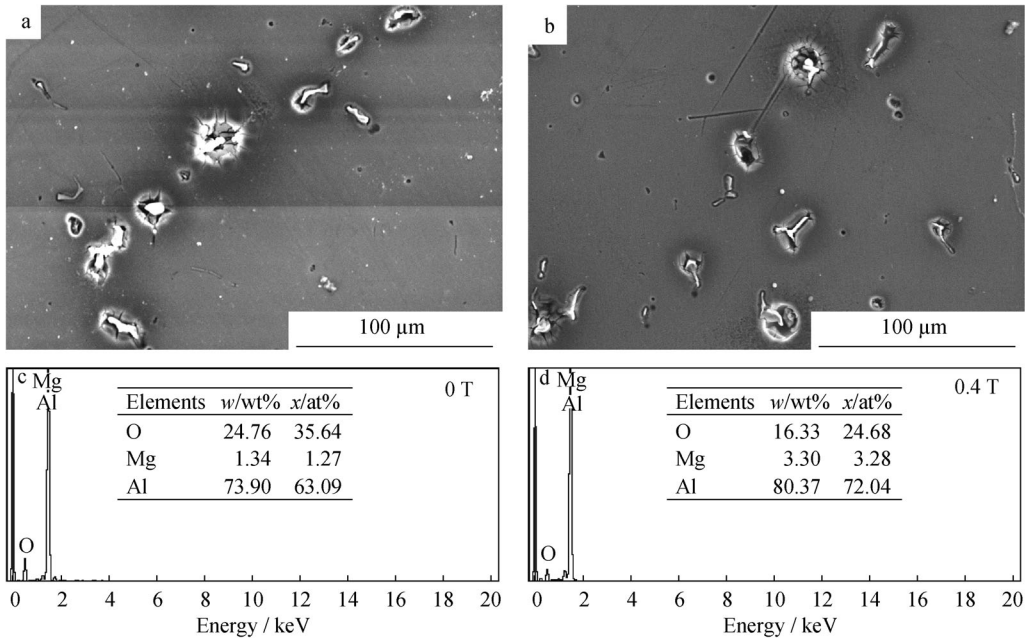

Fig. 9 SEM images and EDS analysis of Al–3.0 wt%Mg alloy immersed in 3.5 wt% NaCl solution for 600 h: **a**, **c** without magnetic field and **b**, **d** with 0.4 T magnetic field

than that of the alloy tested without magnetic field. The corrosion product was analyzed by EDS, as shown in Fig. 9c, d. The corrosion product is composed of the same kinds of elements, oxygen, magnesium and aluminum whether the magnetic field was applied or not. But the content of the elements is different. Oxygen content is reduced from 24.76 wt% to 16.33 wt% when magnetic field was applied during the immersion corrosion test. It means that magnetic field could decelerate the corrosion of Al–3.0 wt%Mg alloy in 3.5 wt% NaCl solution.

The average diameters of the pitting holes on the surface of Al–3.0 wt%Mg alloys corroded in 3.5 wt% NaCl solution were measured, as shown in Fig. 10a. With the increase of immersion time, the diameter of pitting holes increases. In the early stage, the pitting rate of the alloy with magnetic field applied increases, as shown in Fig. 10b. But with the test going on, a passive film is formed progressively on the inner-surface of the pitting holes, and it would impede the growth of pitting holes [20–22]. As a result, the increasing rate of the diameter of pitting holes would slow down gradually and at last comes to a stable value whether the corrosion test was conducted under magnetic field or not. It seems that an applied magnetic field has some effect on enlarging the diameters of pitting holes at the early stage, but it will loss the effect on the corrosion rate of pitting holes after a complete

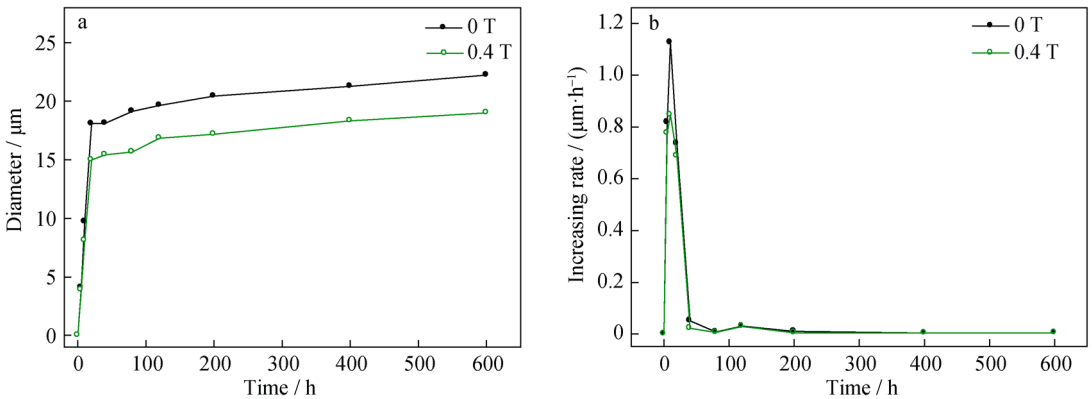

Fig. 10 Pitting hole diameters of Al–3.0 wt%Mg alloys corroded in 3.5 wt% NaCl solution in absence and presence of magnetic field: **a** diameter of pitting holes and **b** increasing rate of diameters of pitting hole

passive film is formed and the pitting corrosion rate comes to a stable value.

4 Discussion

Pitting corrosion is an electrochemical process. It can be described in detail by three very distinguishable steps: breakdown of passive film, early stages of pit growth and repassivation and/or stable pit growth. The corrosion process consists of at least two associated charge transfer reactions: the oxidation of metal (anodic reaction) and the reduction of an oxidizing agent (cathodic reaction). The influences of an applied magnetic field on electrode process of Al–3.0 wt% alloy in 3.5 % NaCl solution are considered to be the effects of activating and dissolving of aluminum anode and process of mass transfer in solution. This effect is produced by magnetohydrodynamic (MHD) flow on metal/solution interfaces due to the existence of an applied magnetic field. Such a MHD flow in an electrochemical system is described by the force per unit volume in solution, $\vec{F}_{\mathrm{MHD}}$:

$$\vec{F}_{\mathrm{MHD}} = \vec{J} \times \vec{B} \tag{4}$$

where $\vec{J}$ is the local flux of ions and $\vec{B}$ is the magnetic field intensity. The directions of ions flux are mainly determined by the electric field in the electrochemical system. So the direction of magnetic field determines the influence of the magnetic field on the mass transfer rate. Specially, $\vec{F}_{\mathrm{MHD}}$ will be the largest when the applied magnetic field is perpendicular to the direction of the ion flux and electric field. In this work, the direction of magnetic field is parallel to the electrode surface. As a result, the applied magnetic field will exert a Lorentz force on any charged particle moving in the interfacial diffusion layer.

Aluminum anodic dissolution could be thought of the following reaction processes [23, 24]. Aluminum dissolution takes place first, losing electron and forming active intermediate $Al^{+}_{(ad)}$ as shown in Reaction (5). Then, unstable $Al^{+}_{(ad)}$ will loss electron and react with H_2O to form Al^{3+} and $Al(OH)_3$ according to Reactions (6) and (7). Reactions (6) and (7) will happen simultaneously. Finally, Al^{3+} will react with Cl^{-}, according to Reactions (8) and (9). This process leads to the dissolution of anodic and the breakdown of passive film. As the result, pitting corrosion will occur.

$$Al - e^{-} \rightarrow Al^{+}_{(ad)} \tag{5}$$

$$Al^{+}_{(ad)} - 2e^{-} \rightarrow Al^{3+} \tag{6}$$

$$Al^{+}_{(ad)} + 3H_2O \rightarrow Al(OH)_3 + H_2 + H^{+} \tag{7}$$

$$Al^{3+} + Cl^{-} + H_2O \rightarrow AlOHCl^{+} + H^{+} \tag{8}$$

$$AlOHCl^{+} + Cl^{-} \rightarrow AlOHCl_2 \tag{9}$$

In the electrochemical process, the movement of electrons and the recombination of ions are involved. One of the reasons for continuing pitting corrosion is a high concentration of aggressive anions within the pitting areas. The precipitation of $AlOHCl_2$ is thought as a main cause to impede the repassivation and maintain the pit corrosion actively. The magnetic field will influence the motion of cations and anions and has an effect on paramagnetic ion which is called "paramagnetic gradient force" as shown in Eq. (10) [25–27].

$$\vec{F}_{\nabla c} = \frac{\chi_{\mathrm{m}} \vec{B}^{2}}{2\mu_0} \vec{\nabla} c \tag{10}$$

where χ_{m} is the magnetic susceptibility, μ_0 is the relative magnetic permeability, $\vec{\nabla} c$ is the concentrations difference of ions between surface and bulk. Under a magnetic field, a gradient of concentration of paramagnetic ions exists due to some electrode reaction in which they participate, and additional driving force acting on them will arise. This force has the same direction as the gradient of the paramagnetic ions, causes a redistribution of velocities in the diffusion layer and increases concentration of paramagnetic ions.

$Al^{+}_{(ad)}$ is formed firstly during the corrosion process of Al–3.0 wt%Mg alloy in 3.5 wt% NaCl solution. The energy of $Al^{+}_{(ad)}$ is so high that $Al^{+}_{(ad)}$ has the electron configuration of $1S^2 2S^2 2P^6 3S^1 3P^1$. It has a single electron in orbit of 3S and 3P each. So, $Al^{+}_{(ad)}$ is a paramagnetic ion and can be attracted by the magnetic field and gather on the surface of aluminum electrode. It will increase the concentration of $Al^{+}_{(ad)}$ on the surface of aluminum electrode and impede the progress of Reaction (5), and then reduce the possibility of the future Reactions (6)–(9). In this case, less electrons and ions, such as Al^{3+}, H^{+}, $AlOHCl^{+}$, are generated to involve into mass transfer and reaction. So, an applied magnetic field would decrease the concentration of ions in diffusion layer and decrease the corrosion current density (i_{corr}) correspondently. A higher pitting corrosion potential and more pit initiation time are needed for Cl^{-} and other ions to breakdown the passive film. It is the reason why the pit initiation time and the pitting corrosion potential increase and corrosion current density decreases in an applied magnetic field, and an applied magnetic field would inhibit the pitting growth of Al–3.0 wt%Mg alloy in 3.5 wt% NaCl solution. Corrosion behavior of Al–3.0 wt%Mg alloy under magnetic field is different from that of other metallic materials in Refs. [5–14]. Although paramagnetic ions exist during the electrochemical reaction

[5–10], the paramagnetic ion in this paper is the intermediate product which would affect later reaction.

5 Conclusion

In this study, the influences of applied magnetic field on the corrosion behavior of Al–3.0 wt%Mg alloy in 3.5 wt% NaCl solution were carried out. The horizontal magnetic field would increase the pitting corrosion potential (E_{pit}) and the charge transfer resistance (R_t) of the tested alloy obviously, and reduce the corrosion current density (i_{corr}) of Al–3.0 wt%Mg alloy in 3.5 wt% NaCl solution. Pitting initiation model of Al–3.0 wt%Mg alloy in 3.5 wt% NaCl solution is changed from A_3 model to $A_3 + A_4$ model when horizontal magnetic field was applied. The magnetic field prolongs the pitting initiation time, slows down the pitting generation rate and depresses the formation of pitting holes of Al–3.0 wt%Mg alloy. The influencing mechanism of all above is that the applied horizontal magnetic field will produce a Lorentz force on any charged particle moving in the interfacial diffusion layer. The force and paramagnetic gradient force would hinder the formation of paramagnetic ion $Al^{+}_{(ad)}$ and reduce the pitting rate.

Acknowledgments This study was financially supported by the National Natural Science Foundation of China (No. 51379070) and the Fundamental Research Funds for the Central Universities (No. 2014B31714).

References

[1] Chung DDL. Electromagnetic interference shielding effectiveness of carbon materials. Carbon. 2001;39(2):279.
[2] Yang SY, Lozano K, Lomel A, Jones R. Electromagnetic interference shielding effectiveness of carbon nanofiber/LCP composites. Compos Part A Appl Sci. 2005;36(5):691.
[3] Kim BR, Lee HK, Park SH. Electromagnetic interference shielding characteristics and shielding effectiveness of polyaniline-coated films. Thin Solid Films. 2011;519(11):3492.
[4] Cui ZH, Zhang C, Jing Y, Liu H, Jia YZ. Influence of alloying elements on corrosion resistance of aluminum alloy foils. Chin J Rare Met. 2014;38(2):176.
[5] Lu Z, Huang C, Huang D, Yang W. Effects of a magnetic field on the anodic dissolution, passivation and transpassivation behaviour of iron in weakly alkaline solutions with or without halides. Corros Sci. 2006;48(10):3049.
[6] Lu Z, Chen JM. Magnetic field effects on anodic polarisation behaviour of iron in neutral aqueous solutions. Br Corros J. 2000;35(3):224.
[7] Sueptitz R, Koza J, Uhlemann M, Gebert A, Schulz L. Magnetic field effect on the anodic behaviour of a ferromagnetic electrode in acidic solutions. Electrochim Acta. 2009;54(8):2229.
[8] Tang YC, Davenport AJ. Magnetic field effects on the corrosion of artificial pit electrodes and thin films. J Electrochem Soc. 2007;154(7):362.
[9] Lu Z, Yang W. In situ monitoring the effects of a magnetic field on the opencircuit corrosion states of iron in acidic and neutral solutions. Corros Sci. 2008;50(2):510.
[10] Su X, Xu GM, Jiang DH. Distribution uniformity of added elements in twin-roll cast Al–Zn–Mg–Cu alloy by multi-electromagnetic fields. Rare Met. 2015;34(8):546.
[11] Hu J, Dong CF, Li XG, Xiao K. Effects of applied magnetic field on corrosion of beryllium copper in NaCl solution. J Mater Sci Technol. 2010;26(4):355.
[12] Guo B, Zhang P, Jin YP, Cheng SK. Effect of alternating magnetic field on the corrosion rate and corrosion products of copper. Rare Met. 2008;27(3):324.
[13] Shinohara K, Aogaki R. Magnetic field effect on copper corrosion in nitric acid. Electrochemistry. 1999;67(2):126.
[14] Chiba A, Ogawa T. Effects of magnetic field direaction on the dissolution of copper, zinc, and brass in nitric acid. Corros Eng. 1988;34(4):455.
[15] Liu L, Li Y, Wang FH. Influence of nanocrystallization on pitting corrosion behavior of an austenitic stainless steel by stochastic approach and in situ AFM analysis. Electrochim Acta. 2010;55(7):2430.
[16] Zhang T, Yang YG, Shao YW, Meng GZ, Wang FH. A stochastic analysis of the effect of hydrostatic pressure on the pit corrosion of Fe–20Cr alloy. Electrochim Acta. 2009;54(15):3915.
[17] Shibata T, Takeyama T. Stochastic theory of pitting corrosion. Corrosion. 1997;33(7):243.
[18] Shibata T, Ameer MAM. Stochastic processes of pit generation on zirconium with an anodic oxide film. Corros Sci. 1992;33(10):738.
[19] Fujimoto S, Shibata T, Minamida M, Udaka S. A statistical evaluation of crevice corrosion on type 304 stainless steel. Corros Sci. 1994;36(9):1575.
[20] Tang YM, Zuo Y, Zhao H. The current fluctuations and accumulated pitting damage of mild steel in $NaNO_2$–NaCl solution. Appl Surf Sci. 2005;243(1–4):82.
[21] Shao M, Fu Y, Hu RG, Lin CJ. A study on pitting corrosion of aluminum alloy 2024-T3 by scanning microreference electrode technique. Mater Sci Eng A. 2003;344(1–2):323.
[22] Arrabal R, Mingo B, Pardo A, Mohedano M, Matykina E, Rodriguez I. Pitting corrosion of rheocast A356 aluminum alloy in 3.5 wt% NaCl solution. Corros Sci. 2013;73:342.
[23] Despić AR. Electrochemical properties of aluminum alloys containing indium, gallium and thallium. J Appl Electrochem. 1976;6(6):527.
[24] Ford FP, Burstein GT, Hoar TP. Bare surface reaction rates and their relation to environment controlled cracking of aluminum alloys. J Electrochem Soc. 1980;127(6):1325.
[25] O'Brien RN, Santhanam KSV. Electrochemical hydrodynamics in magnetic fields with laser interferometry: influence of paramagnetic ions. J Appl Electrochem. 1990;20(3):427.
[26] Hinds G, Coey JMD, Lyons MEG. Influence of magnetic forces on electrochemical mass transport. Electrochem Commun. 2001;3(5):215.
[27] Waskaas M, Kharkats YI. Effect of magnetic fields on convection in solutions containing paramagnetic ions. J Electroanal Chem. 2001;502(1–2):51.